Heliyon 9 (2023) e12958

Contents lists available at ScienceDirect

Heliyon

journal homepage: www.cell.com/heliyon

Research article

Hyperin promotes proliferation, migration, and invasion of HTR-8/SVneo trophoblast cells via activation of JAK1/STAT3 pathway in recurrent spontaneous abortions

Zhenni Mu [a], Sinan Shen [a], Li Tang [a], Yingdie Liu [b], Ziwei Zhou [b], Lei Lei [a,*]

[a] College of Integrated Traditional and Western Medicine, Hunan University of Chinese Medicine, Changsha, China
[b] The First Affiliated Hospital of Hunan University of Chinese Medicine, Changsha, China

ARTICLE INFO

Keywords:
Hyperin
Proliferation
Migration
Invasion
JAK1/STAT3
Recurrent spontaneous abortions

ABSTRACT

The proliferation of extravillous trophoblasts (EVT) and their further migration, invasion, and differentiation into the decidual and myometrial vasculature are vital for spiral artery remodeling. These physiological functions of EVT are also essential steps in the implantation of the human embryo and the formation of the placenta and are closely related to pregnancy maintenance and the occurrence of abortion. Hyperin is a flavonoid with anti-inflammatory, pro-proliferative, and anti-apoptotic properties. Consequently, we investigated the previously unexplored effects of hyperin on the proliferation, migration, and invasion of HTR-8/SVneo cells. Human extravillous trophoblast-derived HTR-8/SVneo cells were incubated with different concentrations of hyperin (0, 5, 10, 25, 50, and 100 μM) to observe the changes in cell proliferation, migration, invasive capacity, and pathway activation. Proliferation, migration, and invasion were promoted by activating the JAK1/STAT3 pathway in HTR-8/SVneo cells treated with hyperin. In addition, brepocitinib (PF-06700841) significantly inhibited the proliferation, migration, and invasion effects of hyperin on HTR-8/SVneo cells. *In vivo* experiments confirmed that hyperin reduces the embryo loss rate in recurrent spontaneous abortion (RSA) model mice. Furthermore, our study revealed that hyperin promoted the proliferation, migration, and invasion of HTR-8/SVneo cells via activation of the JAK1/STAT3 pathway, further improving pregnancy outcomes in RSA.

1. Introduction

Recurrent spontaneous abortion (RSA) is a common complication of female pregnancy, with a prevalence of approximately 1%–5% [1], seriously endangering the reproductive health of women of childbearing age. At present, it is believed that RSA is related to the imbalance of maternal-fetal immune tolerance, and its prevention and treatment are primarily based on aspirin, low-molecular-weight heparin, and other drugs, as well as various active and passive immunotherapies, which have achieved certain clinical efficacy [2]. However, the pathogenesis of RSA is unknown, as is the assessment and diagnosis of maternal-fetal immune tolerance imbalance. The drugs and methods used have only been in use for a short period, the long-term risks are unknown, and the effectiveness of treatment is debatable [3]. Therefore, it is imperative to develop more accurate, safe, and effective methods for assessing and treating RSA.

Human extravillous trophoblast cells (EVT) are important regulatory cells at the maternal-fetal interface that plays a key role in

* Corresponding author.
E-mail addresses: leilei19632021@163.com, 004328@hnucm.edu.cn (L. Lei).

https://doi.org/10.1016/j.heliyon.2023.e12958
Received 25 August 2022; Received in revised form 3 January 2023; Accepted 10 January 2023
Available online 13 January 2023

early embryo implantation and immune regulation [4]. Proper proliferation, migration, and invasion of trophoblast cells are necessary for remodeling spiral arteries, human embryo implantation, and placenta formation. Spiral arterial remodeling is the upward movement of intravascular trophoblasts along the wall of the uterine spiral artery, replacing endothelial cells and disrupting the myometrium, which directly affects pregnancy [5,6]. Trophoblast dysfunction can lead to impaired uterine spiral artery remodeling and adverse pregnancy outcomes, including pregnancy loss, preeclampsia, intrauterine growth restriction, and preterm delivery [4,6].

Hyperin is a natural flavonoid widely distributed in plant fruits and herbs, including Hypericaceae, Erythrinaceae, Labiatae, Rosaceae, Rhododendron, Aconitaceae, Berberidaceae, Garcinia, Fabaceae, and Werspearaceae [7]. Numerous studies have confirmed that hyperin has various biological activities, including anti-inflammatory [8], anti-cancer [9], anti-oxidative stress, and apoptosis [10, 11]. Another study found that hyperin can reduce pregnancy loss in abortive rats by activating autophagy and inhibiting inflammation [12]. However, the mechanism by which hyperin regulates trophoblast function and interferes with pregnancy outcomes in RSA remains unclear. In the present study, we sought to demonstrate the role of hyperin in regulating trophoblast function and verify whether its underlying mechanism is related to the regulation of the JAK1/STAT3 signaling pathway.

2. Materials and methods

2.1. Clinical specimens

Decidual specimens were collected from patients with URSA (n = 3) and from women who had abortions for non-medical reasons (n = 3). All operations were performed between 9:00 a.m. and 11:00 a.m. The exclusion criteria were parental chromosomal abnormalities, anatomical abnormalities, infectious causes, hypertension, diabetes mellitus, heart disease, and thyroid abnormalities. All participants provided written informed consent following the Declaration of Helsinki. This study was approved by the Ethics Committee of the First Affiliated Hospital of Hunan University of Traditional Chinese Medicine.

2.2. Cell culture and maintenance

The human extravillous trophoblast cell line HTR-8/SVneo was acquired from Shanghai Institute of Cell Biology, Chinese Academy of Sciences. HTR-8/SVneo cells were cultured in RPMI 1640 complete medium containing 10% Fetal Bovine Serum (FBS) and 1% penicillin-streptomycin at 37 °C in a 5% CO_2 incubator. The medium was changed every 2–3 days. When the cells reached 80% confluence and were in good condition, the supernatant was discarded, the cells were washed 2–3 times with phosphate-buffered saline (PBS), 1 mL of 0.25% trypsin was added to the culture dish, and the cells were passaged and cultured.

2.3. Animal model

CBA/J mice (24 females, unborn, 6–8 weeks old) and DBA/2 mice (9 males, 6–8 weeks old) were obtained from Beijing Huafukang Biotechnology Co. (NO. SCK2019-0008, Beijing, China). BALB/c mice (three males, 6–8 weeks old) were acquired from Hunan SJA Laboratory Animal Co., LTD (NO. SCK2019-0004, Changsha, China). The animals were housed in the SPF-grade Laboratory Animal Center of Hunan University of Traditional Chinese Medicine at 22 ± 2 °C and 50 ± 5% humidity, with a 12 h light/dark cycle. The experimental protocols were approved by the Animal Experimentation Ethics Committee of Hunan University of Chinese Medicine, China (NO. LL2021032501). Female CBA/J-mated DBA/2J mice comprise a well-known model of pregnancy loss that shares features with human RSA [13-15]. In total, 24 female CBA/J mice were mated with nine male DBA/2 mice and three BALB/c mice in a 2:1 ratio. The former established the RSA mouse model, and the latter established a standard pregnancy mouse model. On the morning following cage mating, the female mice were stained vaginally, and the presence of many sperm on the smear or observation of a mouse vaginal plug was recorded as day 0.5 of pregnancy. Six normal pregnant mice were used as controls. Eighteen RSA model mice were randomly divided into RSA model, dydrogesterone, and hyperin groups. The mice in the blank and RSA model groups were gavaged with 0.2 mL of saline daily, and the mice in the dydrogesterone group were gavaged daily with 4.55 mg/kg/d dydrogesterone tablets (Abbott Healthcare Products BV, USA). In addition, mice in the gentiside group were gavaged with 50 mg/kg hyperin (Shanghai yuan ye Bio-Technology Co., Ltd, China, 482-36-0). All mice were intragastrically administered until 12.5 days of gestation.

2.4. Cell proliferation assay

Cell counting Kit-8 (CCK-8) assay was used to evaluate the proliferation of HTR-8/SVneo cells treated with hyperin. HTR-8/Svneo cells in the logarithmic growth stage were digested with trypsin and counted. The cell density was adjusted to 5×10^4 cells/mL and inoculated in 96-well plates at 100 μL per well. After the cells were plastered, the original cell culture medium was discarded, washed twice with PBS, and incubated with fresh medium containing 0, 5, 10, 25, 50, and 100 μM hyperin for 12, 24, 36, and 48 h. Subsequently, 110 μL of RPMI-1640 reaction solution containing CCK8 (RPMI-1640 medium: CCK8 reagent = 10:1) was added, and the cells were incubated for another 2 h. The absorbance of each well was measured at 450 nm wavelength using a microplate reader (BioTek, USA).

2.5. Western blot (WB) analysis

Tissue or cells were lysed in RIPA lysis buffer (Beyotime, Shanghai, China) containing protease and phosphatase inhibitors,

centrifuged (12500 R/min, 15 min, 4 °C), and the supernatant was extracted. Protein concentration was determined using the BCA Protein Colorimetric Assay Kit (Elabscience, Wuhan, China), and an aliquot of the supernatant was prepared at a concentration of 20 μg/μL of protein supernatant. Equal amounts of protein were separated by SDS-PAGE and transferred to polyvinylidene difluoride (PVDF) membranes (Millipore, USA). The membranes were blocked with 5% skim milk for 1 h at room temperature and incubated with the appropriate antibodies overnight at 4 °C. Subsequently; the membrane was incubated with diluted secondary antibody at 37 °C for 1 h. Finally, the membrane was washed three times with TBST, and the protein bands were analyzed using a Western Blotting Imaging System (ChemiDoc™ XRS+, Bio-Rad, California, USA). The intensities of total JAK1 and total-STAT3 were used as controls for *p*-JAK1 or p-STAT3, respectively, and the intensities of GAPDH were used as controls for all the other bands. Each test was conducted on the same membrane and repeated thrice. The relative expression of the proteins was analyzed using Image Lab software (version 5.2.1 build 11).

The detailed information and dilution ratios of the antibodies were as follows: primary antibodies: anti-phospho-JAK1 (1:1000, Affinity, AF2012), anti-JAK1 (1:1000, Affinity, AF5012), anti-phospho-STAT3 (1:2000, Affinity, AF3293), anti-STAT3 (1:2000, Affinity, AF6294), anti-Ki67 (1:2000, Affinity, AF0198), anti-MCM2 (1:3000, Affinity, AF0206), anti-PCNA (1:3000, Affinity, AF0239), anti-MMP2 (1:2500, Abcam, ab92536), anti-MMP9 (1:2000, Proteintech, 10375-2-AP), and anti-VEGFA (Proteintech, 1:2000, 19003-1-AP); Secondary antibodies: HRP-conjugated Affinipure Goat Anti-Rabbit IgG (H + L) (Proteintech, 1:10000, SA00001-2).

2.6. Reverse transcription and real-time PCR (qPCR)

Total RNA was extracted from tissues or cells using an Ultra-Pure Total RNA Extraction Kit (Simgen, Zhejiang, China) and reverse-transcribed to cDNA using a Reverse Transcription Kit (Novoprotein, Jiangsu, China). The primers were synthesized by Beijing Tsingke Biotechnology Co. (Table 1). qRT-PCR was then performed to amplify the cDNA template using the SYBR qPCR SuperMix Plus Kit (Novoprotein, Jiangsu, China) and the CFX96 real-time PCR System (Bio-Rad, CA, USA). The experiment was repeated thrice. Gene expression was calculated using the $2^{-\Delta\Delta Ct}$ method and normalized to the internal control, GAPDH.

2.7. Wound healing assay

The back of the 6-well plate was marked with three horizontal lines per well. HTR-8/sVneo logarithmic growth cells were digested with trypsin and inoculated into 6-well plates. When the cells had grown to 100% full, the middle of each well was scored vertically with a 1 mL pipette tip, and the cell debris was removed by rinsing 2–3 times with PBS. The corresponding medium was added, and the scratch distance was photographed and recorded under an inverted microscope at 0 and 24 h. The experiment was repeated thrice. The scratch widths were analyzed using ImageJ software (Version 1.53c) to determine the migratory capacity of each group of cells.

2.8. Transwell migration and invasion assay

Cells were digested with trypsin and counted after 24 h of intervention with various drugs for the migration assay. The cells were then resuspended in RPMI-1640 medium without FBS, and the density of the cell suspension was adjusted to 2×10^5 cells/mL. Next, 200 μL of each cell suspension was added to the upper chamber of the Transwell (Corning, USA), and 500 μL of RPMI-1640 medium containing 10% FBS was added to the lower chamber. After 24 h, the cells were fixed in 4% paraformaldehyde for 15 min and stained with 0.1% crystal violet (Beyotime, Shanghai, China) for 20 min. Finally, the number of migrating cells was counted under an inverted microscope (magnification, ×200) in 3 random fields of view.

For invasion assays, the upper chamber of a Transwell system was pre-coated with Matrigel (Corning, USA) before the cells were added. First, Matrigel was melted at 4 °C and diluted 8-fold in RPMI-1640 medium without FBS. Subsequently, 50 μL diluted Matrigel was added into the upper chamber of Transwell and incubated at 37 °C for 1 h. Finally, the cell suspension was added to the upper chamber with Matrigel, and the remaining procedure was the same as for the migration experiment.

2.9. Immunofluorescence assay

2.9.1. Immunofluorescence of cell

HTR-8/sVneo cells in the logarithmic growth stage were digested with trypsin and counted. The cell density was then adjusted to 1×10^4 cells/mL and seeded in 24-well plates containing slides at 1 mL per well. Intervention with different drugs for 24 h after cell

Table 1
PCR primer sequences.

	Forward sequence (5′–3′)	Reverse sequence (5′–3′)
Ki67	CTTTGGGTGCGACTTGACGA	ACAACTCTTCCACTGGGACG
MCM2	GCGAAACCTGGTTGTTGCTG	AGGATTCCGATGATTCCGCC
MMP2	GATACCCCTTTGACGGTAAGGA	CCTTCTCCCAAGGTCCATAGC
MMP9	CATTCAGGGAGACGCCCATT	AACCGAGTTGGAACCACGAC
VEGFA	AGGGCAGAATCATCACGAAGT	AGGGTCTCGATTGGATGGCA
PCNA	GGTTACTGAGGGCGAGAAGC	GACCGGCTGAGACTTGCGTA
GAPDH	AATGGGCAGCCGTTAGGAAA	GCCCAATACGACCAAATCAGAG

adhesion. The medium was then removed, washed with PBS, fixed with 4% paraformaldehyde for 15 min, permeabilized with 0.3% Triton X-100 for 3 min, blocked with PBS containing 1% Bovine Serum Albumin (BSA) for 1 h, and incubated overnight at 4 °C with p-STAT3 (1:200) or STAT3 (1:200) primary antibodies. After subsequent incubation with FITC-labelled secondary antibody for 1 h in the dark, the cells were washed with PBS and incubated with phalloidin (Solarbio, Beijing, China; CA1670) for 15 min at room temperature. After washing with PBS, the cells were mounted on glass slides in the dark using an anti-fluorescence quenching blocker containing DAPI (Solarbio, Beijing, China, S2110). The cells were scanned and imaged under a 40× objective lens using a Panoramic Tissue Cell Quantification System. Five independent fields from the control and different doses of drug-treated cells were photographed, and the fluorescence intensity was measured using ImageJ software (Version 1.53c). To assess the nuclear-to-cytoplasmic fluorescence ratio, a mask in the DAPI fluorescence image was used to identify the nucleus, and a mask in the GFP fluorescence image was used to identify the whole cell. The nuclear-to-cytoplasmic fluorescence ratio = nuclear GFP fluorescence/(whole GFP fluorescence–nuclear GFP fluorescence).

2.9.2. *Immunofluorescence of tissue specimens*

Dewaxed paraffin sections were subjected to antigen repair for 15 min before being closed with goat serum for 30 min and incubated overnight at 4 °C with rabbit primary antibodies against MMP9 (1:200) or STAT3 (1:200) and mouse-derived primary antibodies against human leukocyte antigen-G (HLA-G) (1:200). HLA-G is used as a specific marker of trophoblast cells. Subsequently, FITC-labelled goat anti-rabbit fluorescent secondary antibody (1:300) and Fluor594-labelled goat anti-mouse fluorescent secondary antibody (1:300) were added and incubated for 1 h at room temperature in the dark. Finally, an anti-fluorescence quenching blocker containing DAPI was added to seal the slides. Tissues were scanned and imaged under a 40× objective lens using a Panoramic Tissue

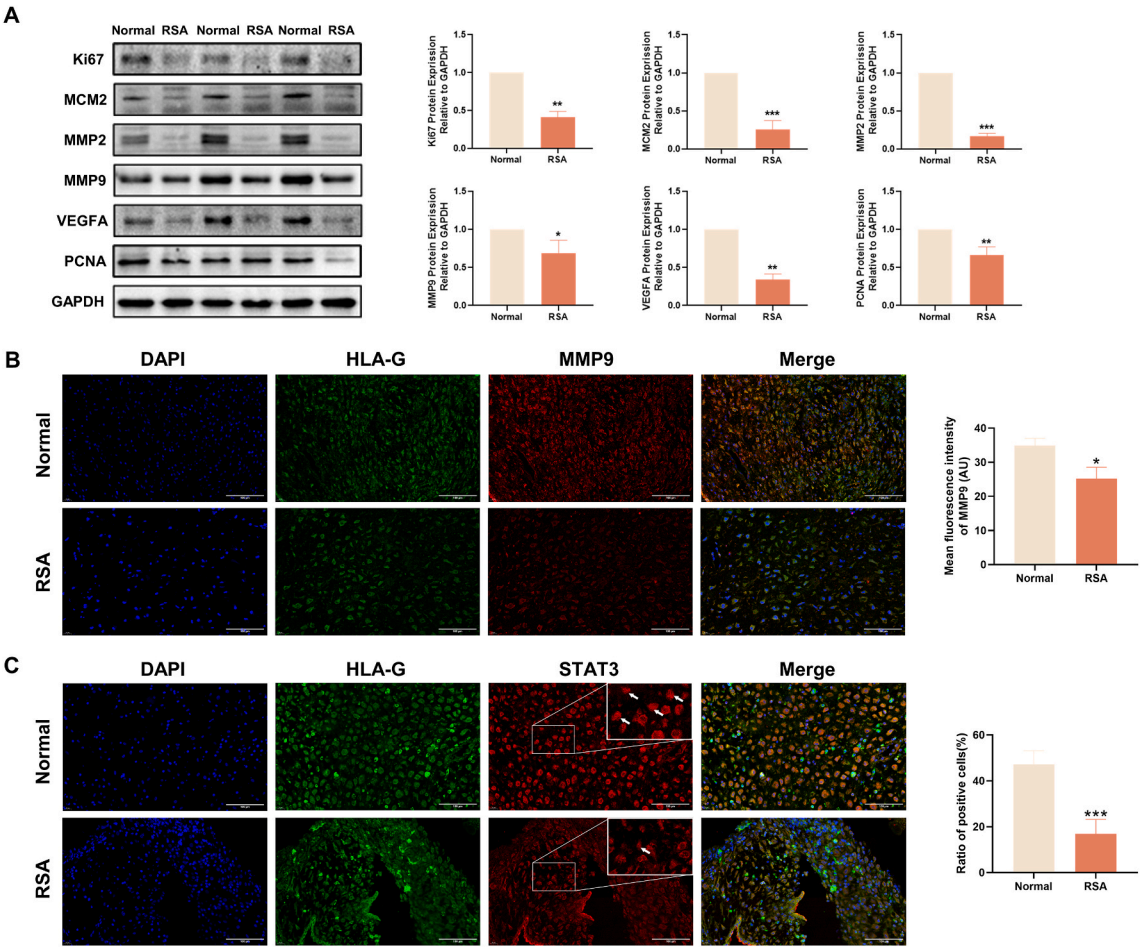

Fig. 1. The expression of factors related to proliferation, migration, and invasion was decreased, and STAT3 activation was inhibited in RSA decidual tissue. (A) The expressions of Ki67, MCM2, MMP2, MMP9, VEGFA, and PCNA in three normal decidual tissues and three RSA decidual tissue were detected using Western blot, and the band intensities were quantified. (B) MMP9 expression in decidual tissue was detected using immunofluorescence (Scale bars, 100 μm), and the mean fluorescence intensity of MMP9 was quantitatively analyzed. (C) STAT3 distribution was detected using immunofluorescence (Scale bars, 100 μm), and ratio of positive cells (STAT3 nuclear translocation) was analyzed. Data represent the means ± SD (n = 3). $^{*}P < 0.05$, $^{**}P < 0.01$, $^{***}P < 0.01$ vs. the normal group.

Cell Quantification System. Five independent fields from normal and RSA decidual tissues were photographed. The mean fluorescence intensity was used to represent the expression of MMP9 and it was measured using ImageJ software (Version 1.53c). The ratio of positive cells with STAT3 nuclear translocation was calculated to determine STAT3 activity. The ratio of positive cells (%) = (number of cells with nuclear translocation/total number of cells) × 100.

2.10. Hematoxylin and eosin staining

Decidual and placental tissues from each group of mice were stained with hematoxylin and eosin (H&E) following standard procedures. The tissues were deparaffinized, rehydrated using ethanol, stained for 5 min using hematoxylin solution, stained for 3 min using eosin solution, rinsed with running water, and mounted by dehydration. Stained images were acquired using a Motic microscopic imaging system.

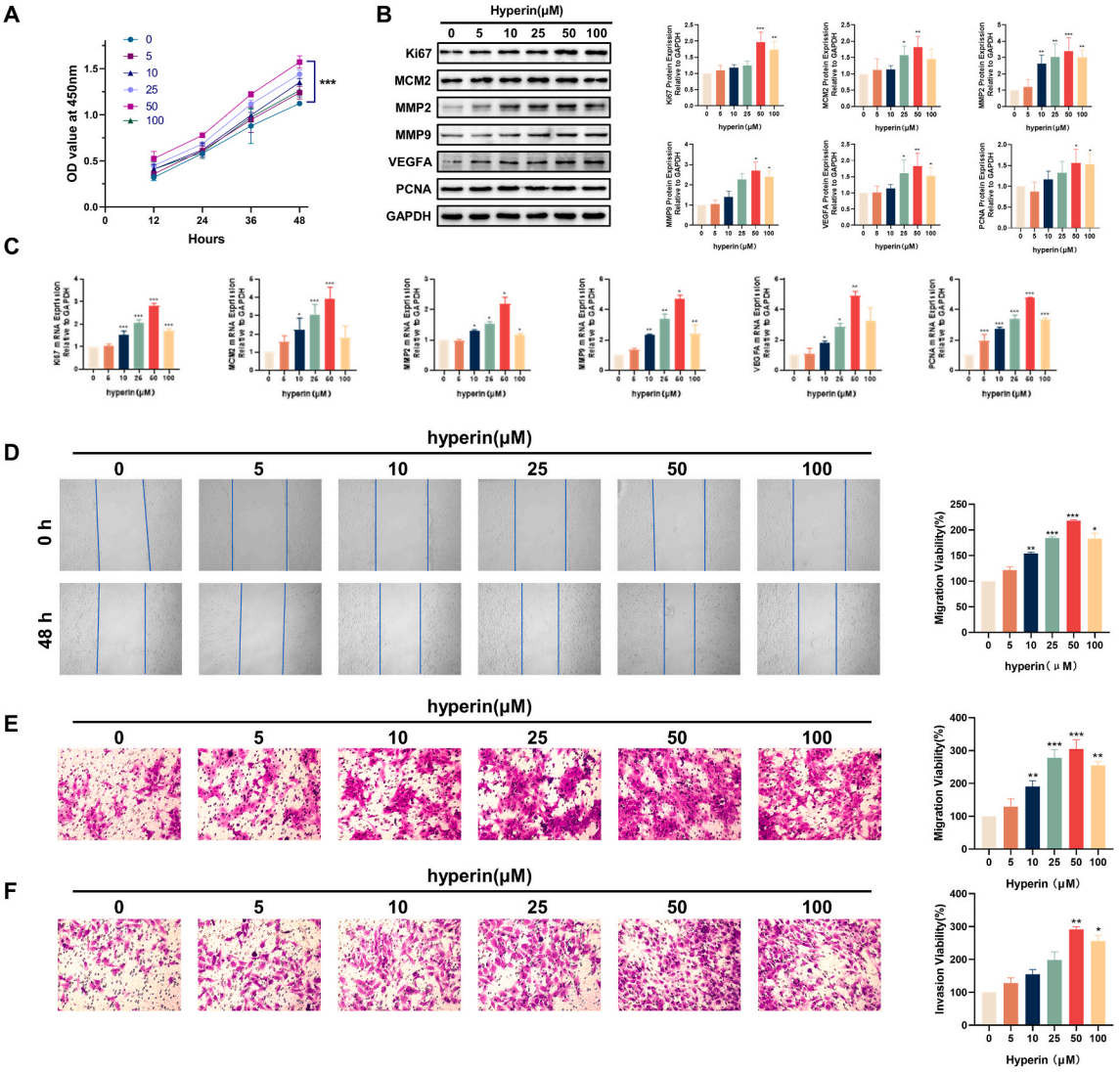

Fig. 2. Hyperin promotes proliferation, migration, and invasion of HTR-8/SVneo cells. (A) The cell viability was measured using a CCK8 assay. (B) The expressions of Ki67, MCM2, MMP2, MMP9, VEGFA, and PCNA were detected using Western blot. (C) The expressions of Ki67, MCM2, MMP2, MMP9, VEGFA, and PCNA were detected using qPCR. (D) Wound healing assay of the migratory ability of HTR-8/SVneo cells after hyperin treatment (50×). Migration viability (%) = {(the initialized width of the scratch) - (the final width of the scratch)}/(the initialized width of the scratch). (E) Cell migration after hyperin treatment was determined by Transwell migration assay (200×). (F) Cell invasion after hyperin treatment was determined by Transwell invasion assay (200×). Data represent the means ± SD from three independent experiments. *$P < 0.05$, **$P < 0.01$, ***$P < 0.01$ vs. the control group.

2.11. Statistical analysis

Quantitative data were expressed as mean ± standard deviation (SD). All statistical analyses were performed using IBM SPSS Statistics for Windows, version 23.0 (IBM Corp., Armonk, N.Y., USA). Significant differences between the two groups were analyzed using the Student's t-test. $P < 0.05$ was considered significantly different.

3. Results

3.1. The expression of factors related to proliferation, migration, and invasion was decreased, and the activation of STAT3 was inhibited in RSA decidual tissue

Matrix metalloproteinases (MMPs) play a crucial role in the invasion of uterine decidua by trophoblasts [16], especially MMP2 and MMP9, which are closely related to pregnancy and abortion [17]. In addition, the nuclear-associated antigen Ki67 (Ki67), proliferating cell nuclear antigen (PCNA), and microchromosome maintenance protein 2 (MCM2) are molecular markers of cell proliferation. Furthermore, vascular endothelial growth factor (VEGF) plays a key role in vasculature formation during embryonic development [18-20]. Western blot analysis revealed that the expression of Ki67, MCM2, MMP2, MMP9, VEGFA, and PCNA decreased in RSA

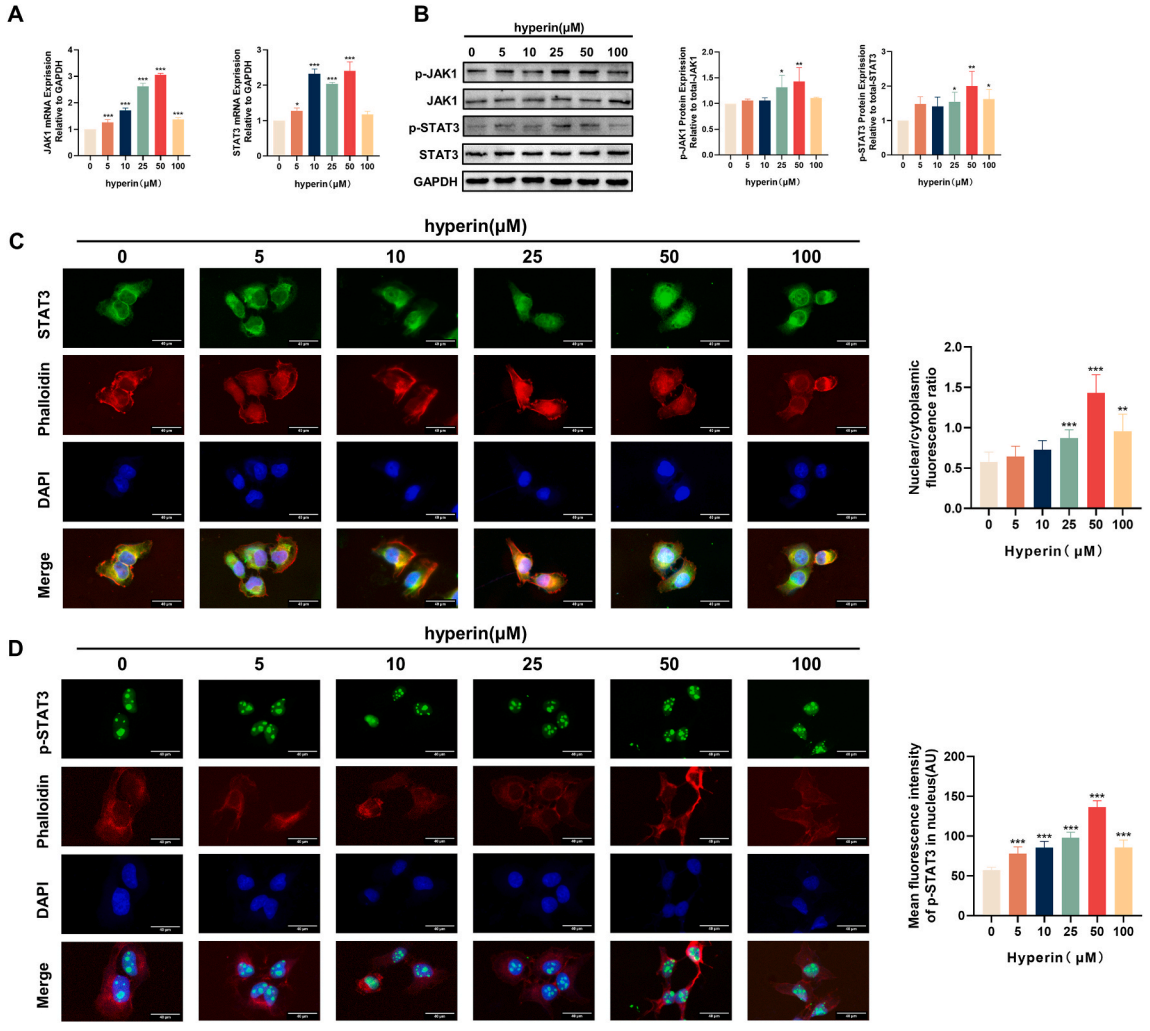

Fig. 3. Hyperin activates JAK1/STAT3 signal pathway in HTR-8/SVneo cells. (A) qPCR detected mRNA expression of JAK1 and STAT3 in HTR-8/SVneo cells. (B) Western blot detected *p*-JAK1/JAK1 and p-STAT3/STAT3 levels in HTR-8/SVneo cells. (C) Nuclear translocation of STAT3 was detected using immunofluorescence in HTR-8/SVneo cells treated with hyperin (Scale bars, 40 μm), and the nuclear-to-cytoplasmic fluorescence ratio was calculated. (D) The p-STAT3 expression in nuclei was detected using immunofluorescence (Scale bars, 40 μm), and the fluorescence intensity was analyzed. Data represent the means ± SD from three independent experiments (600×). $^{*}P < 0.05$, $^{**}P < 0.01$, $^{***}P < 0.01$ vs. the control group.

decidual tissue (Fig. 1A). In addition, we labelled trophoblasts of decidual tissue with HLA-G, stained the nucleus with DAPI, and observed the expression of MMP9 in decidual trophoblast cells. The fluorescence intensity of MMP9 in RSA decidual tissues was lower than that in normal tissues (Fig. 1B).

STAT3 is a key protein that plays a role in transcriptional activation *in vivo* and is a target gene for many important signaling factors. Immunofluorescence analysis revealed that STAT3 was primarily expressed in the cytoplasm of RSA decidual trophoblast cells, whereas STAT3 was expressed in both the nucleus and cytoplasm of normal metaphase cells, indicating that STAT3 activation was inhibited in patients with RSA (Fig. 1C).

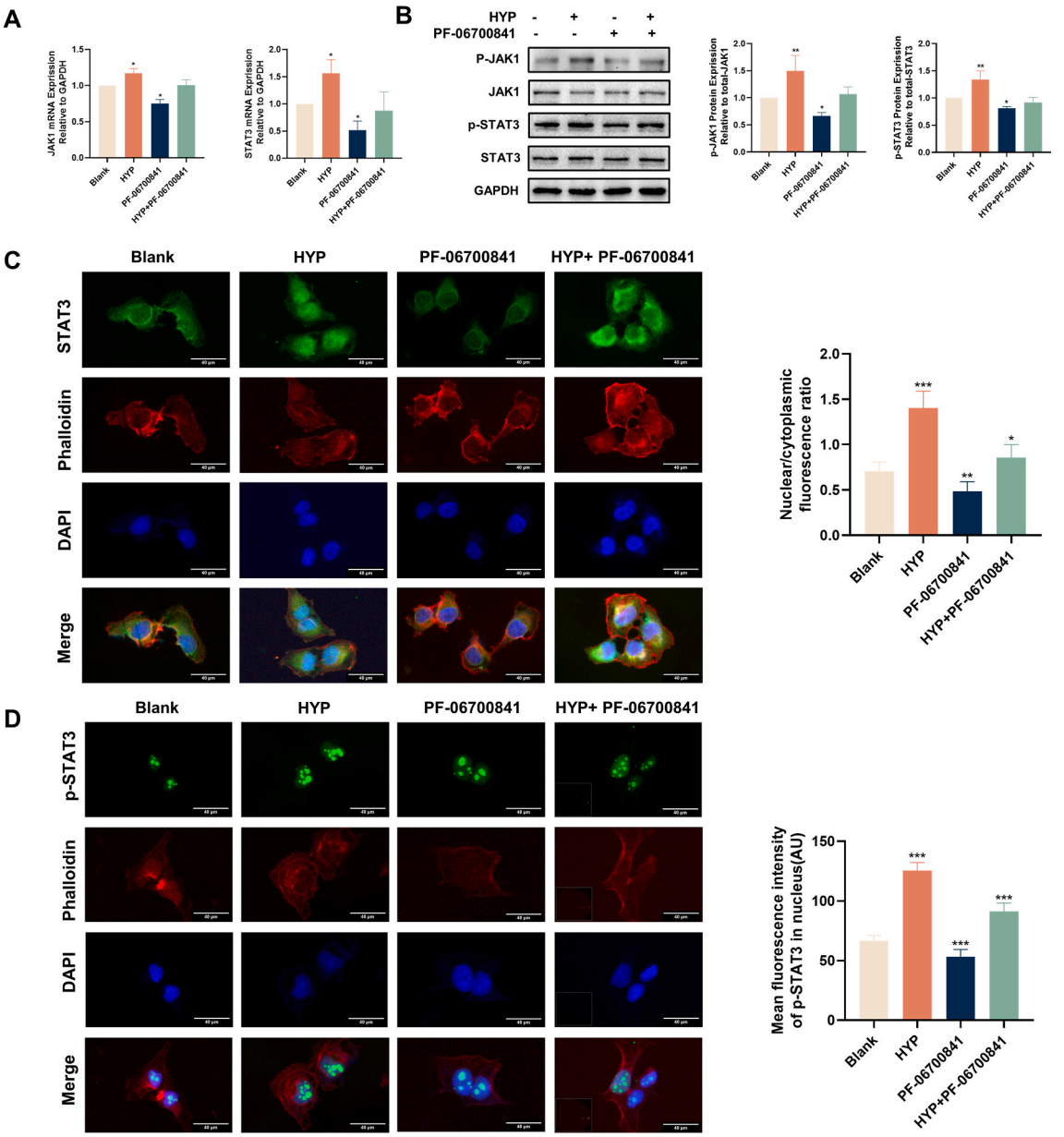

Fig. 4. PF-06700841 inhibits the activation of JAK1/STAT3 pathway by hyperin. (A) qPCR detected mRNA expression of JAK1 and STAT3 in HTR-8/SVneo cells. (B) Western blot detected *p*-JAK1/JAK1 and p-STAT3/STAT3 levels in HTR-8/SVneo cells. (C) Nuclear translocation of STAT3 was detected using immunofluorescence in HTR-8/SVneo cells (Scale bars, 40 μm), and the nuclear-to-cytoplasmic fluorescence ratio was calculated. (D) The p-STAT3 expression in nuclei was detected using immunofluorescence (Scale bars, 40 μm), and the fluorescence intensity was analyzed (600×). $^{*}P < 0.05$, $^{**}P < 0.01$, $^{***}P < 0.01$ vs. the control group.

3.2. Hyperin promotes proliferation, migration, and invasion of HTR-8/SVneo cells

To detect the role of hyperin in HTR-8/SVneo cells, we treated hyperin (0, 5, 10, 25, 50, and 100 μM) in HTR-8/SVneo cells for 12, 24, 36, and 48 h. Here, 0 μM represents the use of only the solvent dimethyl sulfoxide. HTR-8/SVneo cells treated with hyperin demonstrated increased cell viability. After 12 h of treatment, the cell viability of the different groups depicted differences, but the difference was not statistically significant ($P > 0.05$). At the beginning of 24 h of treatment, the cell viability of the hyper in-treated groups (10, 25, 50, and 100 μM) increased significantly ($P < 0.05$), and the difference gradually became obvious over time (Fig. 2A). Next, we treated hyperin (0, 5, 10, 25, 50, and 100 μM) in HTR-8/SVneo cells for 24 h. Western blotting and qPCR were performed to detect the protein and mRNA levels of Ki67, MCM2, MMP2, MMP9, VEGFA, and PCNA, which are associated with proliferation, migration, and invasion. Hyperin treatment promoted the expression of Ki67, MCM2, MMP2, MMP9, VEGFA, and PCNA (Fig. 2B and C). Subsequently, cell migration viability was detected using wound healing and Transwell assays. Hyperin promoted the migration of

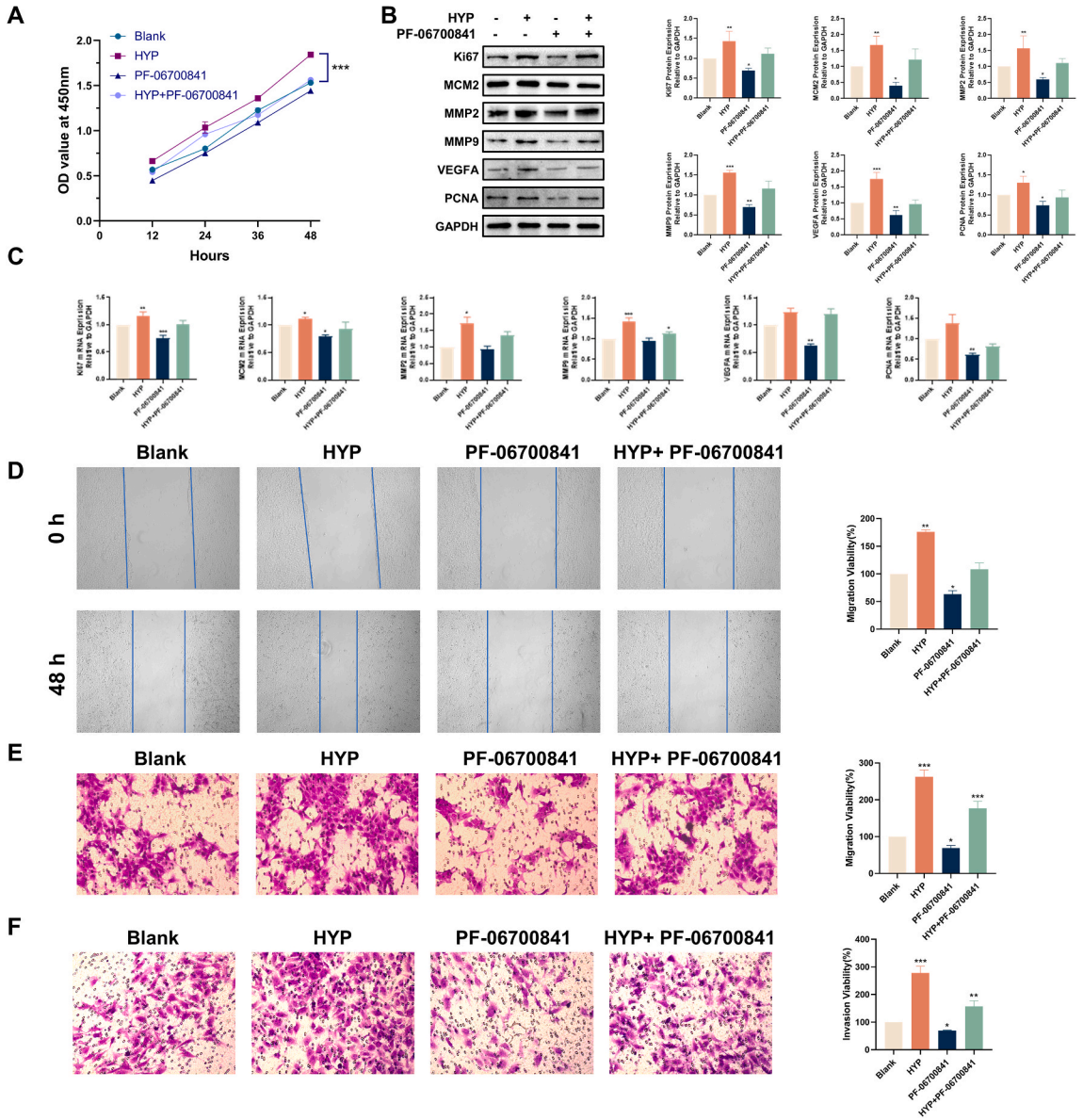

Fig. 5. PF-06700841 inhibits proliferation, migration, and invasion of HTR-8/SVneo cells promoted by hyperin. (A) The cell viability was measured with the CCK8 assay. (B) The expression of Ki67, MCM2, MMP2, MMP9, VEGFA, and PCNA was detected by Western blot. (C) The expression of Ki67, MCM2, MMP2, MMP9, VEGFA, and PCNA was detected by qPCR. (D) Wound healing assay of the migratory ability of HTR-8/SVneo cells after hyperin and PF-06700841 treatment (50×). (E) Cell migration after hyperin and PF-06700841 treatment was determined by Transwell migration assay (200×). (F) Cell invasion after hyperin and PF-06700841 treatment was determined by Transwell invasion assay (200×). Data represent the means ± SD from three independent experiments. *$P < 0.05$, **$P < 0.01$, ***$P < 0.01$ vs. the control group.

HTR-8/SVneo cells (Fig. 2D and E). Meanwhile, invasion ability was detected by the Transwell assay, revealing that hyperin promoted the invasion ability of HTR-8/SVneo cells (Fig. 2F). These results indicate that hyperin promoted the proliferation, migration, and invasion of HTR-8/SVneo cells (Fig. 2).

3.3. Hyperin activates JAK1/STAT3 signal pathway in HTR-8/SVneo cells

The JAK1/STAT3 signaling pathway participates in important physiological processes such as cell proliferation, differentiation, and immune regulation [21] and is one of the pathways involved in the pathogenesis of RSA [22]. Here, we found that hyperin could control the JAK1/STAT3 signaling pathway. HTR-8/SVneo cells were treated with hyperin (5, 10, 25, 50, or 100 μM) for 24 h. Then, the cells were processed for assessment of activated signaling pathways by qPCR, western blotting, and immunofluorescence, as described in the Materials and Methods. The qPCR results demonstrated that the mRNA levels of JAK1 and STAT3 increased with hyperin treatment, and it was most significant when the hyperin concentration was 50 μM and decreased above that concentration (Fig. 3A). Furthermore, western blotting results demonstrated that hyperin induced the phosphorylation of JAK1 and STAT3 (Fig. 3B). Moreover, we stained the cytoskeleton with phalloidin and the nucleus with DAPI, and observed the distribution of STAT3 and p-STAT3 in HTR-8/SVneo cells. Immunofluorescence results revealed that STAT3 was mainly expressed in the cytoplasm of HTR-8/SVneo cells and that p-STAT3 was less distributed in the nucleus in normal HTR-8/SVneo cells. After hyperin intervention,

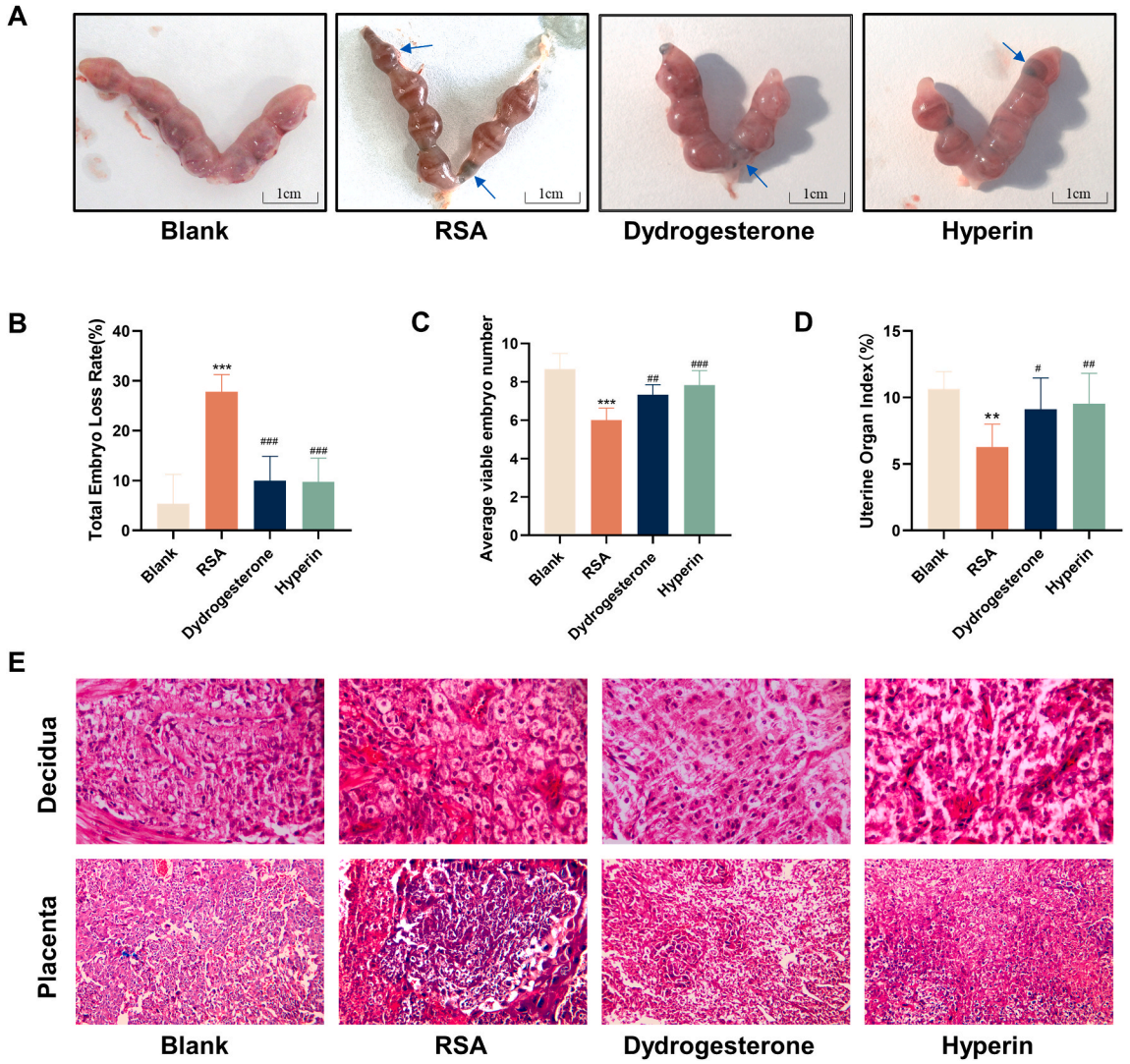

Fig. 6. Hyperin improves pregnancy outcomes in RSA mice. (A) The uterines removed from the mice at 12.5 days of gestation after the treatment of hyperin, dydrogesterone, and control. (B) The total abortion rate was calculated. (C) The average viable embryo number was calculated. (D) The uterine organ index was calculated. (E) H&E staining assay was performed in decidual (200×) and placental tissue (100×). Data are presented as the mean ± SD (n = 6). $^{*}P < 0.05$; $^{**}P < 0.01$; $^{***}P < 0.001$ vs. the blank group; $^{\#}P < 0.05$; $^{\#\#}P < 0.01$; $^{\#\#\#}P < 0.001$ vs. the RSA group.

STAT3 was phosphorylated in the nuclei in large quantities, and the nuclear-to-cytoplasmic fluorescence ratio of STAT3 increased. Moreover, the expression of p-STAT3 in the nuclei increased, and it was most obvious when the hyperin concentration was 50 μM (Fig. 3C and D). Taken together, hyperin could regulate the JAK1/STAT3 signaling pathway (Fig. 3).

3.4. Hyperin promotes proliferation, migration, and invasion of HTR-8/SVneo cells via the JAK1/STAT3 signal pathway

Next, we explored the relationship between hyperin and the JAK1/STAT3 signaling pathway. The cells were treated with hyperin (50 μM) and the JAK1/STAT3 signaling pathway inhibitor brepocitinib (PF-06700841, 20 nM) (MCE, NJ, USA, 1883299-62-4) for 24 h. Subsequently, qPCR and western blotting were performed to detect the mRNA and protein expression of JAK1 and STAT3. The results revealed that hyperin induced JAK1 and STAT3 expression, which was blocked by PF-06700841 (Fig. 4A and B). Furthermore, immunofluorescence was used to detect the distribution of STAT3 in cells and the expression of p-STAT3 in nuclei (Fig. 4B and C). We found that PF-06700841 blocked hyperin-induced activation of the JAK1/STAT3 pathway (Fig. 4). We then evaluated cell viability using a CCK8 assay. We found that PF-06700841 blocked the effects of hyperin on cell proliferation (Fig. 5A). Correspondingly, the mRNA and protein expressions of Ki67, MCM2, MMP2, MMP9, VEGFA, and PCNA were also blocked (Fig. 5B and C). In the meantime, the wound healing assay and the Transwell migration assay were used to confirm the role of hyperin in cell migration. It was shown that PF-06700841 inhibited the effect of hyperin on HTR-8/SVneo cell migration (Fig. 5D and E). Furthermore, the invasion ability detected by the Transwell assay was inhibited by PF-06700841, which was recovered by hyperin (Fig. 5F). In summary, hyperin promotes the proliferation, migration, and invasion of HTR-8/SVneo cells via the JAK1/STAT3 signaling pathway (Figs. 4 and 5).

3.5. Hyperin improves pregnancy outcomes in RSA mice

RSA and standard pregnancy models were established to explore pregnancy outcomes in RSA mice following hyperin treatment. We found that the abortion rate of RSA model mice was reduced, and the number of viable embryos increased after hyperin treatment, achieving a therapeutic effect similar to that of dydrogesterone (Fig. 6A, B, and C). We also calculated the uterine organ index in each group of mice and found that hyperin treatment significantly increased the uterine organ index in the RSA model mice, and the effect was similar to that of dydrogesterone treatment (Fig. 6D). Furthermore, H&E staining demonstrated that the decidual tissue cells were disorganized, the nucleus was fixed and partially disappeared, and the cytoplasm was edematous and partially vacuolated in RSA model mice. In addition, the placenta was loose, the placental cells were arranged disorderly, some cells were hyperplastic and hypertrophied, the cytoplasm was extensively vacuolated, and many inflammatory cells were infiltrated. After intervention with dydrogesterone or hyperin, the cell morphology of the decidua and placental tissue was obviously improved, only a few cells demonstrated edema, and the blood vessels were evenly distributed (Fig. 6E). In summary, hyperin improved the pregnancy outcomes in RSA mice (Fig. 6).

4. Discussion

In this study, we took HTR-8/SVneo cells as the main research object to explore the mechanism of hyperin in treating RSA from the perspective of proliferation, migration, and invasion. We demonstrated that hyperin could improve the pregnancy outcome of RSA, which is manifested in reducing the rate of embryo loss, increasing the number of viable embryos, increasing the coefficient of uterine organs, and improving the pathological morphology of decidua and placenta. It is suggested for the first time that this mechanism may promote the proliferation, migration, and invasion of HTR-8/SVneo cells by mediating the activation of the JAK1/STAT3 signaling pathway.

Damage to spiral artery remodeling caused by functional defects in EVT is now generally considered one of the pathogenic mechanisms of RSA [3]. EVT proliferation, migration, invasion, differentiation into the decidual and myometrial vasculature, and initiation and completion of vascular remodeling are key components in establishing maternal-fetal circulation [5,23], which are crucial for the maintenance of pregnancy. In this study, we found that the expression levels of proliferation, migration, and invasion-related molecules Ki67, MCM2, MMP2, MMP9, VEGFA, and PCNA were lower in the uterine decidual tissues of RSA patients than in the normal group by analyzing the uterine metaplastic tissues of normal miscarriage and RSA patients, indicating that trophoblast function was impaired in RSA patients.

We then studied the effect of hyperin on the proliferation of HTR-8/SVneo cells, as depicted in the results of CCK-8 experiments. In a certain range (concentration <50 μm), hyperin promoted the vitality of HTR-8/SVneo cells in a concentration- and time-dependent manner and enhanced the expression and activity of related molecules, such as Ki67, MCM2, and PCNA. This is consistent with some early research results, which demonstrated that hyperin could promote the proliferation rate of mouse sperm cells [24] and promote the proliferation and differentiation of osteoblasts [25]. However, in some tumor diseases, hyperin inhibits the proliferation of tumor cells [26-29]. These contradictory results indicate that hyperin regulates proliferation in a cell-specific manner.

Studies have demonstrated that proper trophoblast migration and invasion functioning is essential for placental formation and successful pregnancy [30]. Therefore, we demonstrated that hyperin promotes the migration and invasion of HTR-8/SVneo cells and enhances the expression and activity of MMP2 and MMP9. In contrast, Liu et al. [31] found that hyperin inhibited the migration and invasion of lung cancer cells. These contradictory findings indicate that hyperin exerts different regulatory effects on cell migration and invasion under different physiological and pathological conditions. To the best of our knowledge, this is the first study demonstrating that hyperin promotes proliferation, migration, and invasion of HTR-8/SVneo cells.

The JAK/STAT signaling pathway is one of the pathways related to embryo implantation [22] and pregnancy maintenance [32].

Studies have found that the JAK/STAT pathway regulates trophoblast function. For instance, Ankita et al. [33] found that HTR-8/SVneo cells could be induced through the JAK/STAT signaling pathway. Zhao et al. [34] found that EGFR-AS1 could inhibit the proliferation of trophoblasts and induce the disease progression of preeclampsia by inhibiting the JAK/STAT pathway. In this study, we found that the nuclear translocation of STAT3 was inhibited in the EVT of decidual tissues of patients with RSA. Hyperin treatment of HTR-8/SVneo cells promoted the phosphorylation of JAK1 and STAT3 within a certain concentration range, promoted the nuclear translocation of STAT3, and increased the expression of p-STAT3 in the nucleus. Moreover, the regulatory effect of hyperin on HTR-8/SVneo cells was inhibited by the JAK1/STAT3 pathway inhibitor brepocitinib. These results suggest that hyperin regulates the function of HTR-8/SVneo cells through activating the JAK1/STAT3 signaling pathway. Finally, *in vivo* animal experiments verified the improved effect of hyperin on the pregnancy outcome of mice with RSA, which is consistent with previous studies [12].

This study has several limitations. First, we only explored the effect of hyperin on the JAK1/STAT3 signaling pathway, whereas there are other pathways affecting the proliferation, migration, and invasion of HTR-8/SVneo cells. Second, we used normal EVT instead of RSA EVT for the *in vitro* experiments.

In conclusion, our results demonstrated that hyperin promoted proliferation, migration, and invasion of HTR-8/SVneo cells and improved pregnancy outcomes in RSA mice. The pregnancy-protective effect of hyperin may be mediated through the JAK1/STAT3 signaling pathway. Therefore, hyperin may be a promising new therapeutic agent for improving pregnancy outcomes in RSA patients.

Declarations

Author contribution statement

Zhenni Mu: Conceived and designed the experiments; Performed the experiments; Wrote the paper.
Sinan Shen: Performed the experiments.
Li Tang, Ziwei Zhou: Contributed reagents, materials, analysis tools or data.
Yingdie Liu: Analyzed and interpreted the data.
Lei Lei: Conceived and designed the experiments.

Funding statement

This work was supported by Natural Science Foundation of Hunan Province [2021JJ30493], Hunan Province Chinese Medicine Research Program Project [2021007].

Data availability statement

Data will be made available on request.

Declaration of interest's statement

The authors declare no competing interests.

Ethical consideration

This experimental design has been approved by the relevant ethics committee.

Acknowledgements

Thanks to the Home for Researchers for their help in writing this article. Thanks to Hunan province key laboratory of cerebrovascular disease prevention and treatment of intergrated traditional Chinese and western medicine for providing the experimental space.

Appendix A. Supplementary data

Supplementary data related to this article can be found at https://doi.org/10.1016/j.heliyon.2023.e12958.

References

[1] E.G.G.O. Rpl, R. Bender Atik, O.B. Christiansen, et al., ESHRE guideline: recurrent pregnancy loss, Hum. Reprod. Open 2018 (2) (2018), hoy004.
[2] T. Deng, X. Liao, S. Zhu, Recent Advances in treatment of recurrent spontaneous abortion, Obstet. Gynecol. Surv. 77 (6) (2022) 355–366.
[3] S. Zong, C. Li, C. Luo, et al., Dysregulated expression of Ido may cause unexplained recurrent spontaneous abortion through suppression of trophoblast cell proliferation and migration, Sci. Rep. 6 (2016), 19916.

[4] C. Meakin, E.S. Barrett, L.M. Aleksunes, Extravillous trophoblast migration and invasion: impact of environmental chemicals and pharmaceuticals, Reprod. Toxicol. 107 (2022) 60–68.
[5] Y. Sato, Endovascular trophoblast and spiral artery remodeling, Mol. Cell. Endocrinol. 503 (2020), 110699.
[6] K.M. Varberg, M.J. Soares, Paradigms for investigating invasive trophoblast cell development and contributions to uterine spiral artery remodeling, Placenta 113 (2021) 48–56.
[7] Q. Wang, H.C. Wei, S.J. Zhou, et al., Hyperoside: a review on its sources, biological activities, and molecular mechanisms, Phytother. Res. (2022).
[8] F. Liu, Y. Zhao, J. Lu, et al., Hyperoside inhibits proinflammatory cytokines in human lung epithelial cells infected with Mycoplasma pneumoniae, Mol. Cell. Biochem. 453 (1–2) (2019) 179–186.
[9] W. Guo, H. Yu, L. Zhang, et al., Effect of hyperoside on cervical cancer cells and transcriptome analysis of differentially expressed genes, Cancer Cell Int. 19 (2019) 235.
[10] W. Wu, Z. Xie, Q. Zhang, et al., Hyperoside ameliorates diabetic retinopathy via anti-oxidation, inhibiting cell damage and apoptosis induced by high glucose, Front. Pharmacol. 11 (2020) 797.
[11] Y. Zhang, X. Yu, M. Wang, et al., Hyperoside from Z. bungeanum leaves restores insulin secretion and mitochondrial function by regulating pancreatic cellular redox status in diabetic mice, Free Radic. Biol. Med. 162 (2021) 412–422.
[12] A. Wei, Y. Song, T. Ni, et al., Hyperoside attenuates pregnancy loss through activating autophagy and suppressing inflammation in a rat model, Life Sci. 254 (2020), 117735.
[13] A.R. De Fougerolles, M.G. Baines, Modulation of the natural killer cell activity in pregnant mice alters the spontaneous abortion rate, J. Reprod. Immunol. 11 (2) (1987) 147–153.
[14] W.M. Xu, Z.N. Xiao, X.B. Wang, et al., IL-17 induces fetal loss in a CBA/JxBALB/c mouse model, and an anti-IL-17 antibody prevents fetal loss in a CBA/JxDBA/2 mouse model, Am. J. Reprod. Immunol. 75 (1) (2016) 51–58.
[15] S. Bai, B. Huang, S. Fu, et al., Changes in the distribution of intrauterine microbiota may attribute to immune imbalance in the CBA/JxDBA/2 abortion-prone mice model, Front. Immunol. 12 (2021), 641281.
[16] G. Gualdoni, G. Gomez Castro, R. Hernandez, et al., Comparative matrix metalloproteinase-2 and -9 expression and activity during endotheliochorial and hemochorial trophoblastic invasiveness, Tissue Cell 74 (2022), 101698.
[17] Y. Yan, L. Fang, Y. Li, et al., Association of MMP2 and MMP9 gene polymorphisms with the recurrent spontaneous abortion: a meta-analysis, Gene 767 (2021), 145173.
[18] N.N. Chao, J.L. Li, W. Ding, et al., Fabrication and characterization of a pro-angiogenic hydrogel derived from the human placenta, Biomater. Sci. 10 (8) (2022) 2062–2075.
[19] G.W. Aberdeen, J.S. Babischkin, J.R. Lindner, et al., Placental sFlt-1 gene delivery in early primate pregnancy suppresses uterine spiral artery remodeling, Endocrinology 163 (4) (2022).
[20] R.S. Apte, D.S. Chen, N. Ferrara, VEGF in signaling and disease: beyond discovery and development, Cell 176 (6) (2019) 1248–1264.
[21] P. Xin, X. Xu, C. Deng, et al., The role of JAK/STAT signaling pathway and its inhibitors in diseases, Int. Immunopharmacol. 80 (2020), 106210.
[22] Y. Choi, H.R. Kim, E.J. Lim, et al., Integrative analyses of uterine transcriptome and MicroRNAome reveal compromised LIF-STAT3 signaling and progesterone response in the endometrium of patients with recurrent/repeated implantation failure (RIF), PLoS One 11 (6) (2016), e0157696.
[23] A.E. Wallace, R. Fraser, J.E. Cartwright, Extravillous trophoblast and decidual natural killer cells: a remodelling partnership, Hum. Reprod. Update 18 (4) (2012) 458–471.
[24] Y. Zhu, T. Wang, N. Dai, et al., [Hyperoside protects mouse spermatocytes GC-2 cells from oxidative damage by activating the Keap1/Nrf2/HO-1 pathway], Nan Fang Yi Ke Da Xue Xue Bao 42 (5) (2022) 673–680.
[25] J. Zhu, M. Zhang, X.L. Liu, et al., Hyperoside suppresses osteoclasts differentiation and function through downregulating TRAF6/p38 MAPK signaling pathway, J. Asian Nat. Prod. Res. (2022) 1–12.
[26] Y. Kong, W. Sun, P. Wu, Hyperoside exerts potent anticancer activity in skin cancer, Front Biosci (Landmark Ed) 25 (3) (2020) 463–479.
[27] N. Zhang, M.D. Ying, Y.P. Wu, et al., Hyperoside, a flavonoid compound, inhibits proliferation and stimulates osteogenic differentiation of human osteosarcoma cells, PLoS One 9 (7) (2014), e98973.
[28] S. Wei, Y. Sun, L. Wang, et al., Hyperoside suppresses BMP-7-dependent PI3K/AKT pathway in human hepatocellular carcinoma cells, Ann. Transl. Med. 9 (15) (2021) 1233.
[29] M.H. Ping, Hyperin controls the development and therapy of gastric cancer via regulating Wnt/beta-catenin signaling, Cancer Manag. Res. 12 (2020) 11773–11782.
[30] Y. Abbas, M.Y. Turco, G.J. Burton, et al., Investigation of human trophoblast invasion in vitro, Hum. Reprod. Update 26 (4) (2020) 501–513.
[31] Y.H. Liu, G.H. Liu, J.J. Mei, et al., The preventive effects of hyperoside on lung cancer in vitro by inducing apoptosis and inhibiting proliferation through Caspase-3 and P53 signaling pathway, Biomed. Pharmacother. 83 (2016) 381–391.
[32] D.D. Taylor, H.C. Bohler, C. Gercel-Taylor, Pregnancy-linked suppression of TcR signaling pathways by a circulating factor absent in recurrent spontaneous pregnancy loss (RPL), Mol. Immunol. 43 (11) (2006) 1872–1880.
[33] A. Malik, R. Pal, S.K. Gupta, Interdependence of JAK-STAT and MAPK signaling pathways during EGF-mediated HTR-8/SVneo cell invasion, PLoS One 12 (5) (2017), e0178269.
[34] Z.M. Zhao, J. Jiang, Lowly expressed EGFR-AS1 promotes the progression of preeclampsia by inhibiting the EGFR-JAK/STAT signaling pathway, Eur. Rev. Med. Pharmacol. Sci. 22 (19) (2018) 6190–6197.